

# Mechanical and hydraulic properties of nonwoven geotextiles impregnated with asphalt emulsion after damage simulations





*Propriedades mecânicas e hidráulicas de geotêxteis não tecidos impregnados com emulsão asfáltica após simulações de danos*

Mateus Aguiar Lima<sup>1</sup>, Mateus Porto Fleury<sup>1,2</sup>, Jefferson Lins da Silva<sup>1</sup>, Eder Carlos Guedes dos Santos<sup>3</sup>

<sup>1</sup>São Carlos School of Engineering, University of São Paulo, São Carlos, São Paulo, Brasil

<sup>2</sup>Mauá Institute of Technology, São Caetano do Sul, São Paulo, Brasil

<sup>3</sup>School of Civil and Environmental Engineering, Federal University of Goiás, Goiania, Goiás, Brasil

**Contato:** mateuslima@usp.br,  (MAL); mateusfleury@usp.br,  (MPF); jefferson@sc.usp.br,  (JLS); edersantos@ufg.br,  (ECGS)

## Submitted:

12 September, 2022

## Accepted for publication:

18 May, 2023

## Published:

25 August, 2023

## Associate Editor:

Jorge Barbosa Soares  
Universidade Federal do Ceará,  
Brasil

## Keywords:

Geosynthetics.  
Reinforced road.  
Impregnation.  
Durability.  
Reduction factor.  
Asphalt emulsion.

## Palavras-chave:

Geossintéticos.  
Estrada reforçada.  
Impregnação.  
Durabilidade.  
Fator de redução.  
Emulsão asfáltica.

DOI: 10.58922/transportes.v31i2.2809



## ABSTRACT

This study evaluates nonwoven geotextiles' mechanical and hydraulic properties impregnated with asphalt emulsion after simulating installation damage in laboratory conditions. Besides the damage method recommended by ISO 10722, this study considered two static load applications. Two types of nonwoven geotextiles (polyester and polypropylene fibres) were investigated in different conditions regarding i) impregnation with asphalt emulsion, ii) loading condition, and iii) bedding material. The properties evaluated before and after damage consisted of ultimate tensile strength, elongation at break, secant stiffness at 2% strain, and permittivity. The results revealed that the impregnation increased the geotextiles' ultimate tensile strength and secant tensile stiffness but decreased their elongation at break and permittivity. Overall, the geotextiles show good resistance to the installation damage investigated, but after impregnation, the polypropylene geotextile showed to be more sensitive to the damage. The asphalt emulsion composition proved to be important to the geotextiles' properties and response after damage. It can be concluded that the impregnation improved the geotextiles' mechanical properties, but the impregnation effects on the geotextiles' permittivity and resistance to installation damage should be carefully quantified and analysed for design purposes.

## RESUMO

Este estudo avalia as propriedades mecânicas e hidráulicas de geotêxteis não tecidos impregnados com emulsão asfáltica após a simulação de danos de instalação em condições de laboratório. Além do método de dano recomendado pela ISO 10722 (ISO, 2007), este estudo considerou duas aplicações de carga estática. Dois tipos de geotêxteis não tecidos (fibras de poliéster e polipropileno) foram investigados em diferentes condições: i) impregnação com emulsão asfáltica; ii) condição de carregamento/dano; e iii) material de base. As propriedades avaliadas antes e após a simulação dos danos foram resistência à tração, alongamento na ruptura, rigidez secante a 2% de deformação e permissividade. Os resultados revelaram que a impregnação aumentou a resistência à tração e a rigidez à tração secante dos geotêxteis, mas diminuiu o alongamento na ruptura e a permissividade. De modo geral, os geotêxteis apresentaram boa resistência aos danos de instalação investigados, mas, após a impregnação, o geotêxtil de polipropileno mostrou-se mais sensível aos danos.

A composição da emulsão asfáltica demonstrou ser importante para as propriedades e a resposta dos geotêxteis aos danos. Conclui-se que a impregnação melhorou as propriedades mecânicas dos geotêxteis, mas seu efeito sobre a permissividade e a resistência a tração dos geotêxteis aos danos da instalação devem ser cuidadosamente quantificados e analisados para fins de projeto.

## 1. INTRODUCTION

Geotextiles can be widely used in geotechnical projects with single or multiple functions. However, the impacts of upper- and lower-layer materials associated with the compaction process during their installation cause damage that can affect the geotextiles' properties and performance (Izadi et al., 2018). Thus, geosynthetic selection criteria must ensure adequate ultimate tensile strength ( $T_{ult}$ ) values throughout their design life (Pinho-Lopes, Paula and Lopes 2018). To consider the most critical damage/degradation agents in design, Koerner (2005) proposed Equation 1.

$$T_{al} = \frac{T_{ult}}{RF_{ID} \cdot RF_{CR} \cdot RF_D} \quad (1)$$

where:  $T_{al}$ : allowable tensile strength in design;  $T_{ult}$ : ultimate tensile strength of undamaged specimens;  $RF_{ID}$ : reduction factor for installation damage;  $RF_{CR}$ : reduction factor for creep behaviour; and  $RF_D$ : reduction factors due to chemical/biological degradation.

Since the 1990s, the typical approach to identifying  $RF_{ID}$  values has been to simulate in-field installation processes (full scale) and compare the properties of interest (e.g., ultimate tensile strength) before and after damage simulations. This method requires large areas, workload, and heavy equipment, making it extremely time-consuming and expensive. Alternatively, the laboratory test standard ISO 10722 (ISO, 2007) was published to assess the mechanical damage under repeated loading, commonly considered to simulate the geosynthetics' installation damage under controlled conditions.

According to ISO 10722 (ISO, 2007), geosynthetic's samples are confined by a sintered aggregate (aluminium oxide) and subjected to a cyclic load application by a rectangular steel plate in its upper part. Firstly, the confining material is compacted in two stages (pressure of 200 kPa for 60 seconds) in the bottom layer. After arranging the geosynthetic's samples over the bottom layer, the upper one is carefully filled with the confining material avoiding additional damage while spreading it. Finally, the rectangular steel plate applies a cyclic load with values ranging between 5 and 500 kPa, at 1 Hz for 200 cycles. The exhumed damaged samples are tested in the following stage, and the properties of interest are compared to the undamaged samples. Pinho-Lopes and Lopes (2014) observed that the laboratory tests overestimate the installation damage. However, Hufenus et al. (2005) found a good correlation between the laboratory test and the in-situ installation damage. Huang and Wang (2007) proposed how to adequate the load intensity in the laboratory to reproduce the in-field site experimental damage (for flexible geogrids).

The literature has reported different test configurations (geosynthetic or soil types) over the last decades (Hufenus et al. 2005; Carlos et al., 2015; Carlos, Carneiro and Lopes, 2019; Carneiro et al., 2013; Norambuena-Contreras and Gonzalez-Torre, 2015; Zamora-

Barraza et al., 2011; Pinho-Lopes and Lopes, 2014; Gonzalez-Torre et al., 2014). Hufenus et al. (2005) assessed the influence of the geosynthetic's structure, mass per unit area, and confining aggregate over 38 different materials and compared their performance to laboratory damage tests. Carlos et al. (2015) and Carlos, Carneiro and Lopes (2019) evaluated the influence of the grain size distribution (nine soil types) and the mass per unit area of geotextiles on the damage caused by the laboratory tests. In terms of grain-size distribution, the studies reported that the larger the particles are and the more uniform the soil is, the damage induced by the geotextiles tends to be more severe. Although correlations using a physical index (e.g., mass per unit area) with mechanical or hydraulic properties are not recommended (Reinert and Kerry Rowe, 2021), Carneiro et al. (2013) concluded that mass per unit area influences how damage simulations affect geotextile properties.

Considering geosynthetics in contact with bituminous materials, Gonzalez-Torre et al. (2014) investigated the damage according to ISO 10722 (ISO, 2007) and in-field tests. The authors concluded that the secant tensile stiffness is a crucial parameter to be analysed for geosynthetic reinforcing pavement layers, which follows other studies (Pinho-Lopes and Lopes, 2014; Zamora-Barraza et al., 2011; Gonzalez-Torre et al., 2014), and that the ISO 10722 (ISO, 2007) test provides a better repeatability of the results. Several studies (Hufenus et al., 2005; Carlos, Carneiro and Lopes, 2019; Norambuena-Contreras and Gonzalez-Torre, 2015; Pinho-Lopes and Lopes, 2014; Obando-Ante and Palmeira, 2015; Wang et al., 2017; Correia and Zornberg, 2014; Correia, Zornberg and Bueno, 2014) point out that damage during installation induces changes during geosynthetic performance, and the laboratory simulation method helps to understand and forecast how it will happen in the field. Based on the studies mentioned, laboratory tests'  $RF_{ID}$  values range between 1.02 and 9.93.

When roads are constructed using nonwoven geotextiles combined with asphalt concrete, it is essential to impregnate them with asphalt binders to improve their adherence to the adjacent layers (Koerner, 2005; Obando-Ante and Palmeira, 2015). Modifiers added to asphalt products may enhance specific properties (e.g., stability, stiffness, elongation, durability). Therefore, applying asphalt binders to dry, clean, and well-compacted surfaces is highly recommended (Wang et al., 2017). In an innovative study, Correia, Zornberg and Bueno (2014) found that an amount of asphalt emulsion equal to the geosynthetic retention capability improves mechanical performance. It also reduces hydraulic conductivity (Correia and Zornberg, 2014). However, there is a lack of assessing the effect of asphalt emulsion (present in the cracked overlay or the new overlay) on the geosynthetics' installation damage. Thus, the ISO 10722 (ISO, 2007) standard can be a suitable alternative to investigate the installation damage of geotextiles impregnated with asphalt emulsion when applied as a reinforcement element in pavement rehabilitation.

Applying a bituminous layer over impregnated geotextile is a way to reinforce low-traffic roads using an alternative for low-cost pavements. This method applies the impregnated geotextile directly over a subgrade or base layer after surface compaction and shaping. The lack of studies on this application and the evaluation of geotextile damage during the installation procedure have motivated this investigation.

## 2. MATERIALS AND METHODS

### 2.1. Geotextiles and impregnation method

This study investigated two needled-punched nonwoven geotextiles commonly applied to reinforce pavement: one manufactured with polyethylene terephthalate (PET; Figure 1a) and another with polypropylene (PP; Figure 1b). Another selection criterion was the geotextiles' mass per unit area ( $\mu_a$ ). Since nonwoven geotextiles with  $\mu_a$  higher than 200 g/m<sup>2</sup> have shown insufficient impregnation effectiveness (Koerner, 2005; Wickert, 2003), the study adopted materials with  $\mu_a$  equal to 150 g/m<sup>2</sup>. Table 1 shows the geosynthetics' physical and mechanical properties and the asphalt emulsions' characteristics (the adopted test methods are also presented).

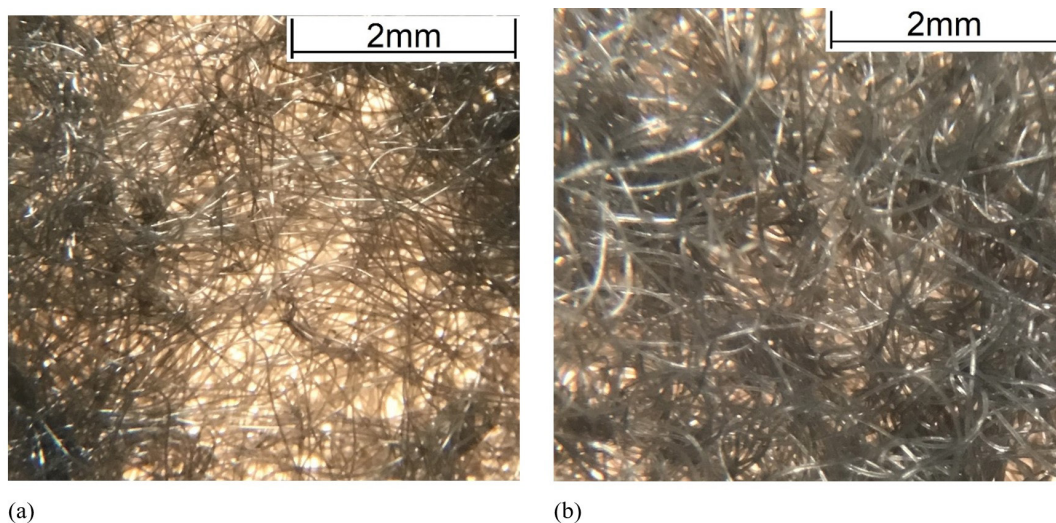


**Figure 1.** View of the structures of geotextiles tested: a) PET and b) PP yarns.

**Table 1:** Nonwoven geotextiles' properties and characteristics of the asphalt emulsion

Geotextiles' properties	Specification	Unit	PET <sup>(1)</sup>	PP <sup>(1)</sup>	
Nominal thickness	ASTM D5199 (ASTM, 2012)	mm	1.562 (9.1)	1.894 (10.5)	
Mass by unit area	ASTM D5261 (ASTM, 2018)	g/m <sup>2</sup>	142 (5.8)	165 (12.6)	
Ultimate tensile strength	ASTM D5035 (ASTM, 2011)	kN/m	5.47 (13.9)	6.14 (11.6)	
Elongation at break	ASTM D5035 (ASTM, 2011)	%	59.7 (2.5)	75.8 (8.3)	
Permittivity	ASTM D4491 (ASTM, 2017a)	s <sup>-1</sup>	5.29 (3.0)	2.39 (10.1)	
Asphalt emulsions' characteristics	Specification	Unit	GTX	CRS-1	CRS-1S
Viscosity Saybolt-Furol	ASTM D7491 (ASTM, 2017b)	s		10.0	19.0
Residue by evaporation	ASTM D6934 (ASTM, 2016)	%		47.9	60.9
Specific mass	-	g/L		1013.16	752.04
Penetration grade	ASTM D5/D5M (ASTM, 2013)	dmm		140.0	63.0
Asphalt retention rate	ASTM D6140 (ASTM, 2005)	g/m <sup>2</sup>	PET	1.69	1.52
			PP	1.61	1.44

(<sup>1</sup>) Coefficient of variation (COV), in percentage, between parentheses.

The geotextile impregnation intends to improve its adherence to adjacent layers, and a reduction in the material permittivity ( $\Psi$ ) is expected. The impregnation process followed one of the approaches recommended by the ASTM D6140 (ASTM, 2005). The nonwoven

geotextile samples (obtained directly from the manufacturer's rolls) were dipped in a large amount of asphalt emulsion (until reaching their impregnation) and then air-dried for 24 hours to ensure emulsion hardening.

The study has investigated six impregnation conditions. The first two conditions consisted of the geotextiles under non-impregnated conditions (PET-0 and PP-0). The other ones comprise both geotextiles impregnated with two asphalt binders (PET-1, PET-1S, PP-1 and PP1-1S). Both asphalt binders are cationic asphalt emulsions of rapid setting (CRS-1 and CRS-1S) and were used as provided by the manufacturer. The CRS-1 consists of a straight-run asphalt emulsion, while the CRS-1S was the same CRS-1 emulsion but modified with the polymer SBS (styrene-butadiene-styrene) – modification process performed by the manufacturer. As the CRS-1 has a higher specific mass than CRS-1S (due to the difference in asphalt content proportion presented in each emulsion), the modified emulsion has left a higher amount of residue after the impregnation process. The asphalt retention rates (property that quantifies the geotextile's capacity to retain the asphalt emulsion) obtained following ASTM D 6140 (2005) for each combination of asphalt emulsion are shown in Table 1.

## 2.2. Damage materials

To represent in-situ work conditions, this study used two natural materials for damage simulation: i) sand (SA) and ii) silty clay (SC). Figure 2 shows both materials' grain-size distribution curves compared to the standard one. These two materials (SA and SC) were adopted in the bottom layer of the experiment to assess how the lower layer could influence the geotextiles' properties after damage (once geotextiles are conventionally arranged between different aggregates in pavement structure). SA was oven-dried before the damage tests, and SC was prepared with moisture content equal to 21.5%.

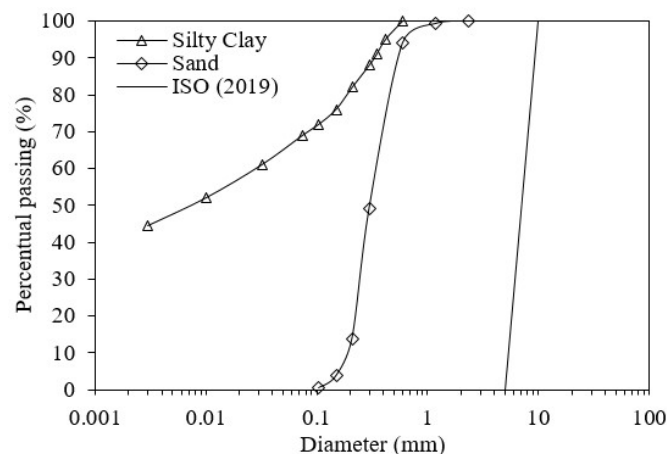


Figure 2. Grain size distribution of the granular materials and the one recommended by ISO 10722.

## 2.3. Damage simulation

This study investigated three loading conditions: i) cyclic loading (CC), ii) short-static loading (SS), and iii) long-static loading (LS). The CC condition followed the ISO 10722 (ISO, 2007) loading method (cyclic load ranging from 5 to 500 kPa at 1 Hz frequency for 200 loading cycles). The SS condition comprised an applied load of 200 kPa for 60 seconds over the loading plate

area. Finally, the LS condition applied a load of 120 kPa (maximum value due to the risk of damaging the air-pressure bag) over the upper granular material for 120 seconds.

Depending on the type of loading method applied in each scenario, a specific box was used to perform the damage simulations: i) a square box for the cyclic (CC) and short-static (SS) load applications and ii) a rectangle box for the long-static (LS) loading. The square box used in this study was larger than the one established by ISO 10722 (ISO, 2007), therefore the loading plate and geotextiles samples were scaled to maintain a proportional condition. The square box had the dimensions of 500 mm (long)  $\times$  500 mm (wide)  $\times$  250 mm (high). The load application plate was 333 mm (long)  $\times$  167 mm (wide), and it was placed centralised to the box and the geotextile sample. Due to the dimensions of the rectangle box – 1,500 mm (long)  $\times$  700 mm (wide)  $\times$  250 mm (high) – three samples were tested simultaneously. An air-pressured bag was used to apply the load over the area of the rectangular box.

The damage tests were conducted using sand on the upper layer for all scenarios investigated. The SC was compacted as recommended by ISO 10722 (ISO, 2007) and reached a compaction degree of 88.6%. The SA was placed into the test box and reached a relative density close to 70.0%. The schemes of both boxes used in this study are shown in Figure 3. The short-static (SS) loading condition was only investigated for the geotextiles under non-impregnated conditions. The other loading procedures (LS and CC) were investigated testing all six impregnation conditions.

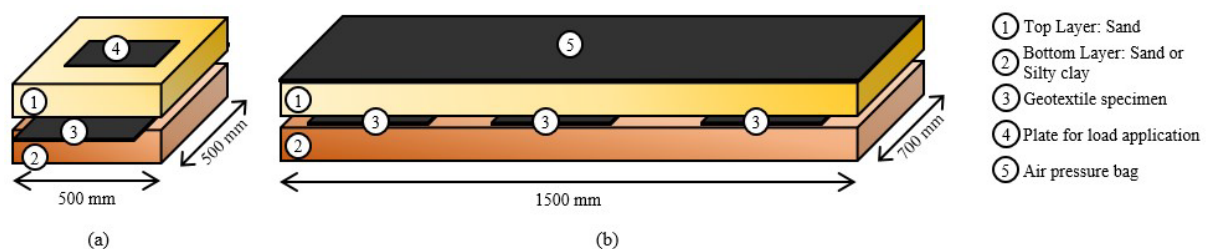


**Figure 3.** Scheme of the damage equipment: (a) square box: short-static (SS) and cyclic (CC) load applications, and (b) rectangle box: static-load (SL) application.

## 2.4. Damage quantification

The damage quantification occurred by assessing the geotextile mechanical and hydraulic properties before and after the damage simulations. Each nonwoven geotextile sample provided five specimens (50-mm wide and 200-mm long) for the tensile strength test and four (80-mm diameter specimens) for the permittivity test. The specimens were maintained during 24 hours in the testing room (before testing) provide a uniform temperature during testing - room temperature of  $22 \pm 2$  °C. The standard ASTM D5035 (ASTM, 2011) was used to measure the ultimate tensile strength ( $T_{ult}$ ), elongation at break ( $\epsilon_{rup}$ ), and the secant tensile stiffness at 2% of elongation ( $J_{2\%}$ ). Tensile tests were performed (five specimens for each scenario) using a universal testing machine with a load cell of 30 kN and a strain rate of 10%/min. Pneumatic jaw clamps were used to ensure that no slipping occurs during loading enabling the strain measurement based on

the top clamp displacement. The permittivity ( $\Psi$ ) was measured following the ASTM D4491 (ASTM, 2017a) recommendations, using the falling head test method.

To quantify the damage caused due to the laboratory simulations, a confidential interval was established for each property of interest ( $T_{ult}$ ;  $\epsilon_{rup}$ ;  $J_2\%$ ; and  $\Psi$ ) using the Student's t-distribution statistical analysis. The confidential intervals were calculated for the non-damaged samples under the non-impregnated and impregnated (with CRS-1 or CRS-1S) conditions. The maximum and minimum value of a property of interest were determined based on Equation 2.

$$X_{max} \text{ or } X_{min} = X_v \pm \frac{t \cdot s}{\sqrt{n}} \quad (2)$$

where:  $X$ : property of interest;  $X_{max}$ : maximum value of the property of interest;  $X_{min}$ : minimum value of the property of interest;  $X_v$ : mean value of the property of interest;  $s$ : sample's standard deviation;  $n$ : sample size; and  $t$ : Student's t-distribution variable.

The confidential interval indicates the range of values representing each property of interest in its undamaged condition. Thus, a damaged scenario that resulted in a mean value inside its respective confidential interval indicates doubt about damage occurrence as it can be considered inside the variability of the undamaged scenario. Otherwise, values outside the confidential interval indicate a significant change in the property's mean value due to the damage simulation investigated in the scenario.

Reduction factors for installation damage ( $RF_{ID}$ ) were also calculated based on the results of the ultimate tensile strength ( $T_{ult}$ ) and the Student's t-distribution statistical analysis. For mean damaged values inside or above the confidential interval, an  $RF_{ID}$  equal to 1.00 was attributed. For mean damaged values below the confidential interval, the  $RF_{ID}$  was calculated as follows (Equation 3):

$$RF_{ID} = \frac{T_{ult\_und}}{T_{ult\_d}} \quad (3)$$

where:  $T_{ult\_und}$ : mean undamaged ultimate tensile strength; and  $T_{ult\_d}$ : mean damaged ultimate tensile strength.

### 3. RESULTS AND DISCUSSION

In this section, the results were summarised in figures where the vertical columns indicate the mean value of the analysed property of interest, and the error bars represent the samples' maximum and minimum values (for the same property). The horizontal dashed lines indicate the confidential interval of each geotextile based on the results obtained with the reference specimens tested (undamaged non-impregnated, or undamaged impregnated) and the Student's t-distribution statistical analysis. Unfortunately, the PET geotextile specimens tore during the test in the scenario PET-0-SA-SS, which means non-impregnated PET geotextile was tested with SA on the bottom layer and submitted to the SS loading condition.

### 3.1. Ultimate tensile strength ( $T_{ult}$ )

The impregnation significantly increased (between 40.6% and 117.8%) the mean  $T_{ult}$  value of undamaged non-impregnated specimens (Figure 4a). The increases occurred regardless of the geotextile type and asphalt emulsion. The asphalt emulsion inside the geotextiles' structure acts as an extra binder between the fibres (beyond the bonds caused by the fibres interweaving and its friction) and enhances the geotextile's strength. The improvement of the PET geotextile's  $T_{ult}$  values found in this study (66.5% for CRS-1 emulsion and 40.6% for CRS-1S emulsion) are close to the ones reported by Correia, Zornberg and Bueno (2014) – values between 40 and 62%. Unexpectedly, even with the smallest asphalt retention rates (Table 1), PP geotextile exhibited an increase of 117.8% and 82.4% when impregnated with the CRS-1 and CRS-1S, respectively.

Figure 4a also indicates that the non-modified asphalt emulsion (CRS-1) increased  $T_{ult}$  values more than the modified asphalt emulsion (CRS-1S). Due to the incorporated polymer (SBS), the CRS-1S emulsion exhibited less specific mass, and after the impregnation process, it was evident that this emulsion (CRS-1S) had difficulty incorporating into the geotextiles – leaving more residues after the impregnation process, as previously mentioned (Section 2.1). The difficulty of CRS-1S to incorporate into the geotextile structure, identified by the lower asphalt retention rate of CRS-1S compared to CRS-1 (Table 1), validates this assumption.

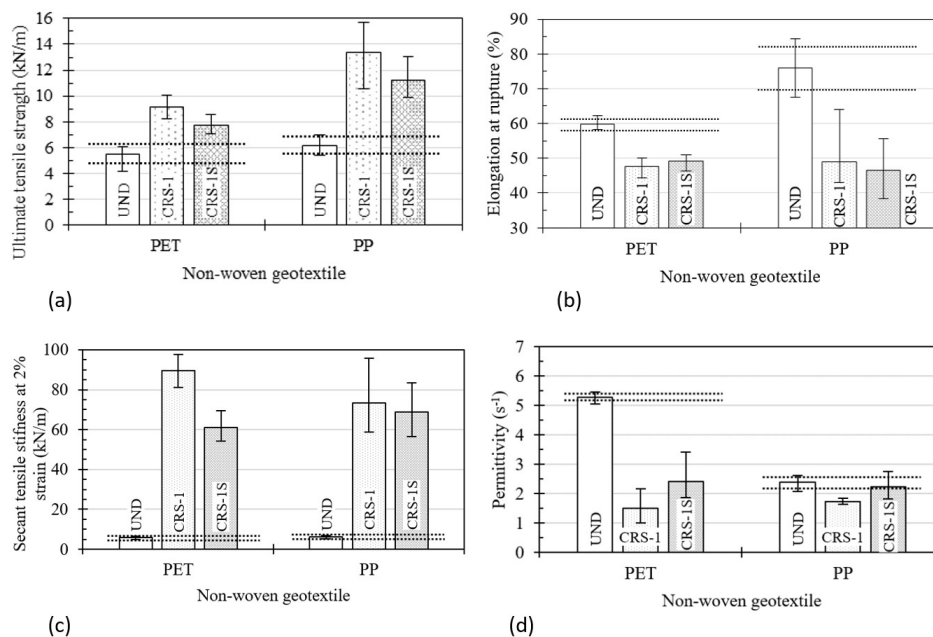


**Figure 4.** Changes in the (a) ultimate tensile strength, (b) elongation at rupture, (c) secant-tensile stiffness at 2% strain, and (d) permittivity after impregnation process.

For the PET geotextile, a damaged mean  $T_{ult}$  value below the material's confidential interval (indicated by the horizontal lines in Figure 5a) occurred when the specimens were tested in the PET-0-SC-CC scenario (reduction of 13.7% compared to the mean  $T_{ult}$  value of undamaged non-impregnated specimens). In the case of the PP geotextile, the reduction below its undamaged non-impregnated confidential interval only occurred for



the PP-0-SA-LS scenario (decrease of 18.0%). These results rise from the high variability of the geotextiles' mean  $T_{ult}$  values ( $COV$  values higher than 11.5% for both materials) and the slight decreases caused by the damage procedures. The discussion of the results shown in Figures 3b, 3c, and 3d are presented in the following sections (3.2, 3.3, and 3.4).

As shown in Figure 5a, the installation damage did not cause significant changes to the undamaged geotextiles'  $T_{ult}$  mean values. The results reported in the literature (Hufenus et al., 2005; Pinho-Lopes and Lopes, 2014), using the standard material for ISO 10722 (ISO, 2007) (a sintered aggregate; aluminium oxide), have shown a significant decrease in this parameter from undamaged to ones obtained by this study. The sharp grain-format and stiffness of the sintered aggregate result in a more aggressive confining material. Moreover, the dimension of the particles used in the study is smaller than the minimum size of corundum particles (see Figure 2).

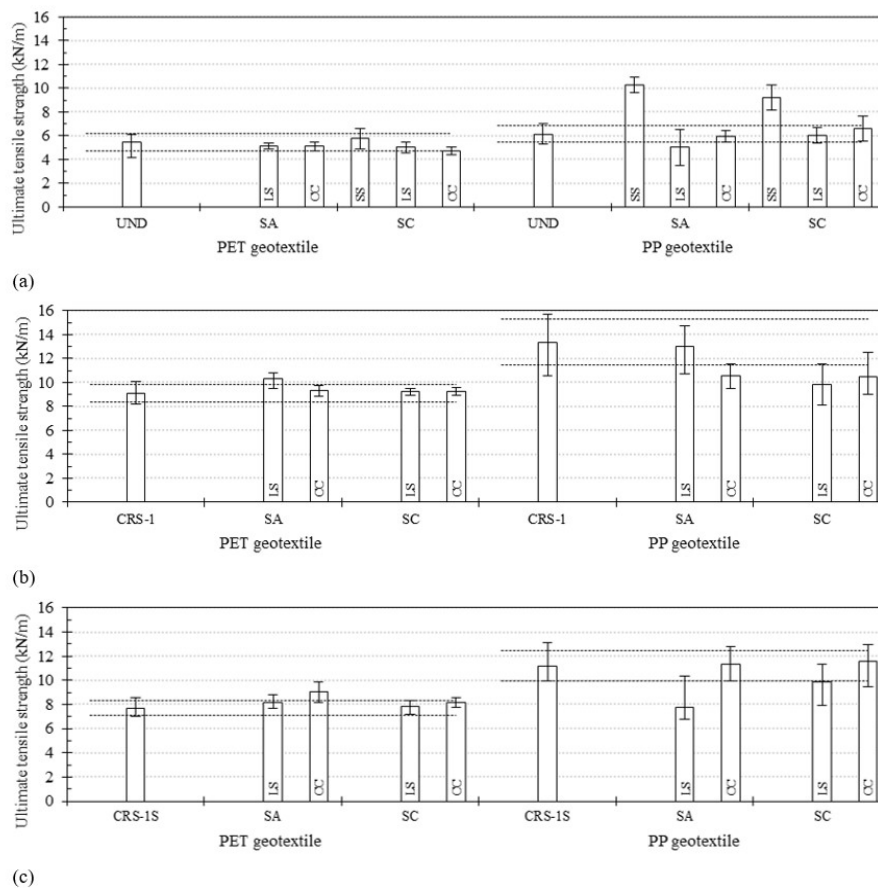


**Figure 5.** Ultimate tensile strength after the installation damage procedures under a) non impregnated condition, b) impregnated with CRS-1 and c) CRS-1S asphalt emulsions

Considering the short-static (SS) loading condition, the damaged PP geotextile specimens experienced a significant increase (higher than 50.0% regardless of the material present in the bottom layer – SA or SC) in the mean  $T_{ult}$  value compared to the undamaged non-impregnated one (Figure 5a). Other studies related to geosynthetics' durability also exhibited this phenomenon, which has been explained by: i) the specimens' storage and temperature condition before testing (Kondo et al., 1992; Rowe, Rimal and Sangam, 2009), ii) a possible

rearrangement of the geosynthetic fibres (Paula, Pinho-Lopes and Lopes, 2004; Ching-Chuan and Shuay-Luen, 2006) and iii) a strain hardening phenomena caused by the damage procedures (Allen and Bathurst, 1994). Possibly, the higher loading stress (200 kPa) applied for 60 seconds (SS condition) was able to compress the geotextile's structure and may enhance the friction between the fibres, increasing its strength. Similar results were found by Domiciano, Santos and Silva (2020) for geogrids tested under higher confining stresses (300 and 600 kPa applied for 300 seconds). This phenomenon may not occur under lower confining stress (120 kPa) and when applied for a shorter period (120 seconds; LS condition).

The results of the impregnated specimens submitted to installation damage simulation are present in Figures 4b and 4c for the CRS-1 and CRS-1S asphalt emulsion, respectively. As can be seen, under the impregnated condition, the PP geotextile is more sensitive to the damage investigated than the PET geotextile. The impregnated PET geotextile specimens did not present a reduction (below the confidential interval) in its undamaged impregnated  $T_{ult}$  mean value for all scenarios investigated regardless of i) the material present in the bottom layer (SA or SC), ii) the loading condition (CC or LS), and iii) the asphalt emulsions. The loading conditions (CC or LS) may have made the PET geotextile structure (comprised of the fibres and the asphalt emulsion) more compacted and increased its strength. Further studies of the physical characteristics of damaged impregnated samples are required to confirm the aforementioned assumption.

The impregnated PP geotextile has shown some scenarios with a mean  $T_{ult}$  value smaller than its undamaged impregnated confidential interval. When impregnated with CRS-1 (Figure 5b) and tested with SC in the bottom layer, the PP geotextile's  $T_{ult}$  mean value reduced by 21.5% and 26.5% for the CC and LS conditions, respectively. The reduction in the  $T_{ult}$  mean value caused by the SA in the PP geotextile impregnated with CRS-1 was equal to 21.2% for the CC condition, and it was negligible for the LS condition (2.9%). Considering the modified asphalt emulsion (CRS-1S; Figure 5c), only the LS condition caused significant changes in the impregnated  $T_{ult}$  mean value of the PP geotextile: a reduction of 31.0% was experienced when tested confined by SA, and the SC in the bottom layer resulted in a decrease of 12.2% of  $T_{ult}$ .

There is a significant difference between the results obtained for PP geotextile when impregnated with CRS-1 and CRS-1S. The geotextile flexibility after the impregnation may explain these results. The higher asphalt pavement rate obtained with the CRS-1 emulsion makes the geotextile structure less flexible and reduces the capacity to absorb the effort caused by the damage process. On the other hand, after being impregnated with the CRS-1S asphalt emulsion, the structure of the PP geotextile remained flexible and could absorb the load from the CC condition. The PET geotextile possibly did not exhibit the same behaviour as it proved more resistant to installation damage.

### 3.2. Elongation at rupture ( $\epsilon_{rup}$ )

After the installation damage under non-impregnated condition, both geotextiles experienced reductions in their mean  $\epsilon_{rup}$  values below the confidential interval of the undamaged non-impregnated specimens (Figure 6a). The PET geotextile experienced higher decreases in the  $\epsilon_{rup}$  values than the PP geotextile (except when tested confined by SA under the LS condition). For this property, the CC condition showed to be the most

aggressive loading condition, followed by the SS and LS conditions, in this order – regardless of the geotextile investigated. The  $\varepsilon_{rup}$  values of the impregnated PET geotextile were more affected when the SC was present in the bottom layer.

Even under the impregnated condition, the geotextiles kept on experiencing a reduction in its mean  $\varepsilon_{rup}$  values after damage (Figures 5b and 5c). The CC loading condition proved to be more aggressive to this property (reductions ranging from 16% to 35%) than the LS loading condition (reductions ranging from 6% to 25%). It can be noted that the level of reduction of  $\varepsilon_{rup}$  when the geotextiles were impregnated are similar to the reduction experienced by the geotextiles under non-impregnated conditions. Unlike the damaged non-impregnated specimens, the mean  $\varepsilon_{rup}$  value of the PP geotextile specimens was more affected than the PET geotextile ones (for most of the evaluated scenarios), similar to the results reported by Fleury et al. (2023).

### 3.3. Secant tensile stiffness at 2% strain ( $J_{2\%}$ )

The geosynthetic's secant tensile stiffness is another important parameter when analysing its mechanical performance for pavement application. Both nonwoven geotextiles presented similar results of  $J_{2\%}$  for undamaged specimens (PET = 5.8 kN/m and PP = 5.4 kN/m). The impregnation enhanced the values of  $J_{2\%}$  approximately by ten times compared to the undamaged specimens, revealing values higher than 60 kN/m (Figure 4c). Both geotextiles experienced a similar improvement in the  $J_{2\%}$  value, but when impregnated with CRS-1,  $J_{2\%}$  was slightly greater (increases of 1250% and 1453% for PP and PET, respectively) than with CRS-1S asphalt emulsion (increases of 1169% and 959% for PP and PET, respectively). These results rose due to the bonding between the asphalt emulsion and the geotextile structure, increasing the overall stiffness. The impregnation increased the mechanical properties of nonwoven geotextiles mainly at low elongation levels, which is crucial for pavement applications.

After the installation damage procedures, the mean  $J_{2\%}$  values significantly increased (above the materials' confidential interval for this property) for the CC and SS loading conditions (Figure 7a). The LS loading condition was responsible for significantly decreasing the analysed property after the damage in non-impregnated specimens. Interestingly, for this loading condition, the material in the bottom layer has minimal importance as each geotextile exhibited a very similar reduction (17.7% and 52.2% for the PET and PP ones).

When impregnated, the geotextiles experienced similar results to those under non-impregnated conditions. The LS loading can be considered the most aggressive condition as all mean  $J_{2\%}$  values were smaller than those obtained after the CC loading condition, and it resulted in some mean  $J_{2\%}$  values smaller than the geotextiles confidential interval (Figures 6b and 6c). The scattered results obtained did not enable us to identify which material present in the bottom layer is the most aggressive and which asphalt emulsion provides better resistance to the installation damage procedures.

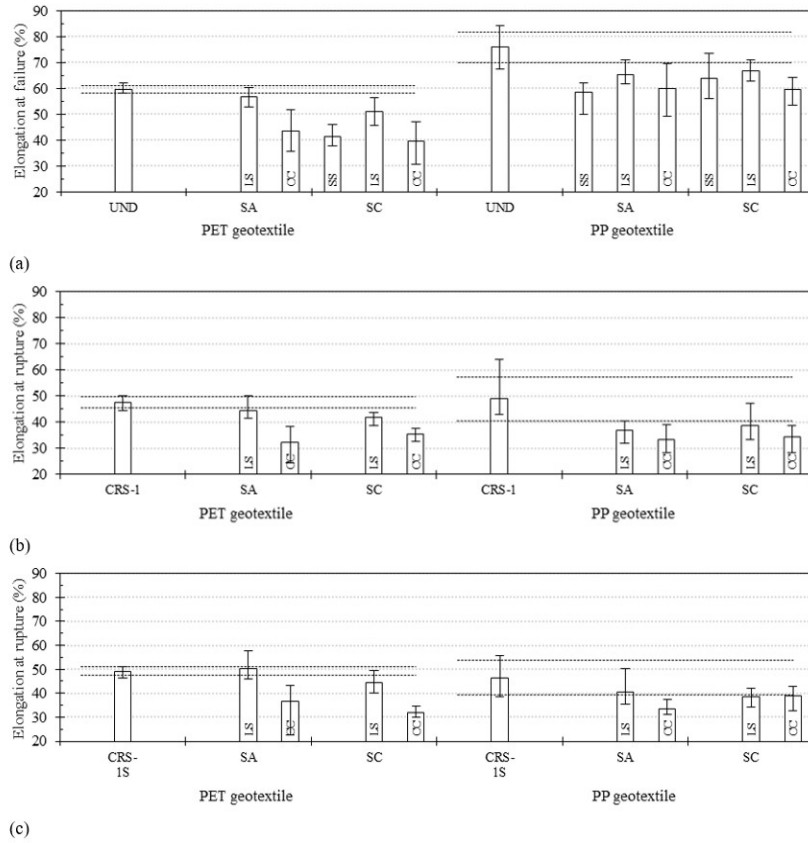


**Figure 6.** Elongation at rupture after the installation damage procedures under a) non impregnated condition, b) impregnated with CRS-1 and c) CRS-1S asphalt emulsions.

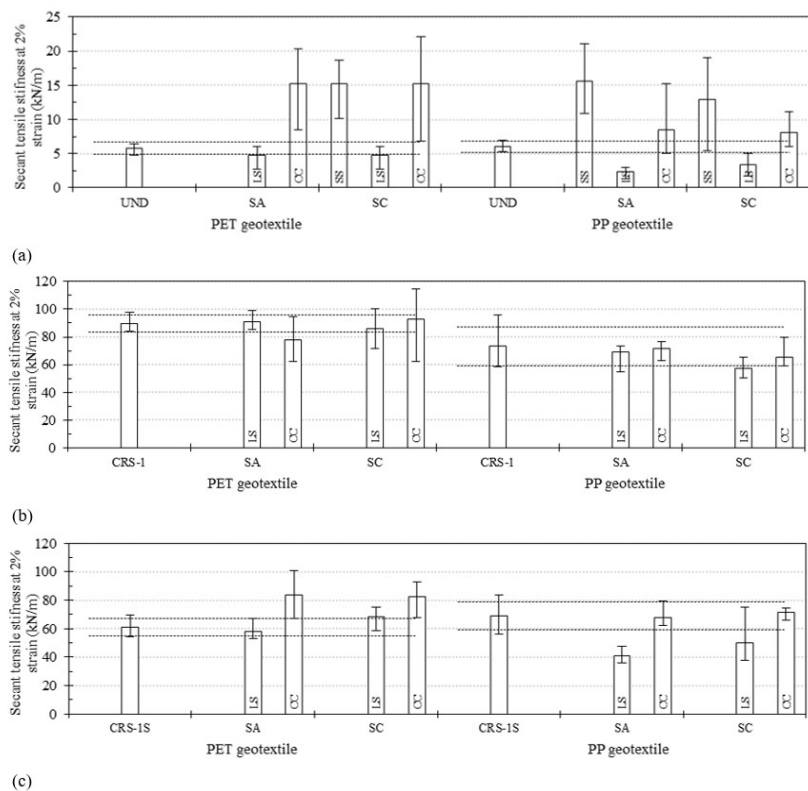


**Figure 7.** Secant tensile stiffness at 2% strain after the installation damage procedures under a) non impregnated condition, b) impregnated with CRS-1 and c) CRS-1S asphalt emulsions.

### 3.4. Permittivity ( $\Psi$ )

After the impregnation, the asphalt emulsion tends to fill the voids in the geotextiles' structures and reduces their permittivity ( $\Psi$ ; Figure 4d). It was observed that PET geotextile specimens experienced more impact than the PP specimens: CRS-1 and CRS-1S decreased the PET geotextile permittivity by 71.3% and 58.8%, respectively. On the other hand, PP geotextile permittivity was also reduced, showing a significant difference for each asphalt emulsion adopted. CRS-1S did not cause substantial changes (reduction of 6.7%) in the geotextile's  $\Psi$  value as the mean value was within the confidential interval of the undamaged non-impregnated specimens. The less adherence capability of this asphalt emulsion to the PP geotextile (confirmed by the smallest asphalt retention rate value in Table 1) can be considered the reason for these results. A reduction of 27.6% occurred in the PP geotextile  $\Psi$  when CRS-1 was used.

The specimens impregnated with the CRS-1S presented mean  $\Psi$  values higher than those impregnated with CRS-1. Due to the difficulty of CRS-1S to incorporate into the geotextile structure (as previously mentioned in Section 3.1) the specimens impregnated with this asphalt emulsion have more voids in their structure, resulting in a more permittivity structure (compared to the impregnated with CRS-1). Moreover, it must be pointed out that the variability in the  $\Psi$  values obtained with CRS-1S were higher than the ones obtained with CRS-1. Under the impregnation with CRS-1S emulsion, due to the nonwoven geotextiles' heterogeneous structure, the emulsion may have better adherence where there are agglomerated fibres, inducing a high variability in the permittivity values. Due to the better CRS-1 adherence, this effect was not so expressive. Further studies are required to validate this assumption.

Considering the adoption of impregnated geotextiles between the surface course (or binder course) and the base layer, when the pavement is not in contact with water, the decrease in the permittivity will not affect the pavement performance. However, when the water seeps into the pavement through cracks in its surface, the smaller permittivity of the impregnated geotextile may contribute to water accumulation (increase the pore-water pressure when the pavement is loaded) and accelerate the development rate of cracks due to pumping. For this reason, the designers must be encouraged to quantify and analyse if the reduction in the geotextile's permittivity after the impregnation can compromise the pavement performance.

An increase in mean  $\Psi$  values can be expected after the installation damage procedures since the rupture of the fibres may occur with local damage that open the geotextile structure. However, the installation damage affected the permittivity of the geotextiles in different ways (Figure 8). The non-impregnated PET geotextile exhibited close reductions in the undamaged mean  $\Psi$  values regardless of the material in the bottom layer and loading condition (ranges between 14.2% and 21.9%; Figure 8a). Moreover, the tests performed with SC in the bottom layer have resulted in slightly higher damage than those confined by SA.

After damage under the impregnated condition, the PET geotextile presented mean  $\Psi$  values inside its confidential interval (except for the scenario PET-1S-SC-CC; reduction of 36.3%). It is worth mentioning that the confidential intervals obtained for impregnated PET geotextile is very wide as this property exhibited a huge variability when

impregnated (28.4% and 33.6% for CRS-1 and CRS-1S asphalt emulsions, respectively). In the case of the PP geotextile, different permittivity results were observed for each asphalt emulsion. When impregnated with CRS-1S, all scenarios resulted in a reduction close to 17.6% (except for PET-1S-SA-LS). When impregnated by CRS-1, the results showed discrepant behaviours, sometimes increasing or decreasing the permittivity.

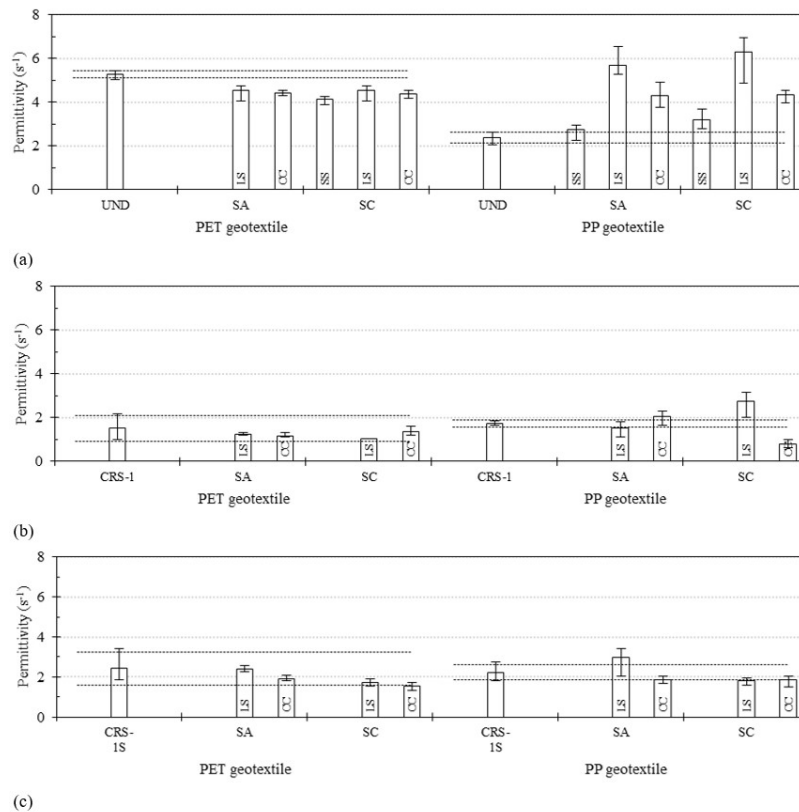


**Figure 8.** Permittivity after the installation damage procedures under a) non impregnated condition, b) impregnated with CRS-1 and c) CRS-1S asphalt emulsions.

### 3.5. Reduction factors

A quantitative way to consider the damage when designing with geotextiles, impregnated or not, is by computing the reduction factors obtained from damage simulations tests performed in laboratory conditions. Table 2 shows the reduction factors for installation damage ( $RF_{ID}$ ) related to the ultimate tensile strength ( $T_{ult}$ ) following the methodology described in Section 2.4. It is worth mentioning that the  $RF_{ID}$  reported in the present study can be taken as a reference in design if the field condition applies the same materials used in the research and the same compaction effort.

Table 2 shows a predominance of values equal to 1.00. As previously mentioned in Section 3.1, values lower than those obtained using the standard material (10722 ISO, 2007) can be expected due to the sintered aggregate's high aggressive characteristics (format and stiffness). However, the  $RF_{ID}$  values obtained in the present study were also lower than the ones obtained by Pinho-Lopes and Lopes (2014) and by Hufenus et al. (2005) considering the results related to non-woven geotextiles of both studies, which tests were performed with natural aggregates. The grain size distribution curve may be

the reason for these different results since the test conditions of such studies were quite the same – following ISO 10722. The RFID values are also lower than the ones presented by Gonzalez-Torre et al. (2014) testing geotextile with the same mass per unit area and the aggregate recommended by ISO 10722 (ISO, 2007).

**Table 2:** Reduction factors for installation damage – related to the ultimate tensile strength – for the scenarios evaluated

Impregnation condition	Confined Material	Loading condition	PET	PP
Non-impregnated	Sand	CC	1.00	1.00
		LS	1.00	1.05
		SS	N.T	1.00
	Silty Clay	CC	1.16	1.00
		LS	1.00	1.00
		SS	1.00	1.00
Impregnated with CRS-1	Sand	CC	1.00	1.27
		LS	1.00	1.00
	Silty Clay	CC	1.00	1.28
		LS	1.00	1.36
Impregnated with CRS-1S	Sand	CC	1.00	1.00
		LS	1.00	1.45
	Silty Clay	CC	1.00	1.00
		LS	1.00	1.14

Note: CC, cyclic load; LS, long-static load; SS, short-static load; PET, poly(ethylene) terephthalate; PP, polypropylene; N.T, not tested.

## 5. CONCLUSION

This study reported laboratory installation damage performed in geotextiles under non-impregnated and impregnated (with asphalt emulsion) conditions. Results of tensile and permittivity tests performed in virgin and exhumed specimens have led to the following conclusions:

- The asphalt emulsion intruded into the geotextile structure, and it makes the impregnated geotextile stiffer and less flexible after the drying period. As a result, the geotextiles increased their ultimate tensile strength and secant tensile stiffness. These increases caused a loss in deformability. As the asphalt emulsion (inside the voids) tore during the tensile test, some adjacent fibres also tore, decreasing the elongation at rupture. In terms of permittivity, a significant decrease occurs since the voids of the structure are filled with asphalt emulsion. Moreover, the modifier (polymer SBS) proved to decrease the asphalt emulsion's adherence to the geotextile and affects the properties after impregnation. The effects of the asphalt emulsion with the modifier (polymer SBS) on the impregnated geotextiles' properties were smaller than the ones obtained with the non-modified asphalt emulsion.
- Under the impregnated condition, the PET geotextile maintained its resistance to the installation damage. Unexpectedly, the PP geotextile presented to be more sensitive after impregnation. It shows scenarios with a significant decrease in the ultimate tensile strength leading to reduction factors between 1.14 and 1.45. However, in most scenarios, the geotextiles exhibited values inside the reference value's confidence interval, leading to a reduction factor equal to 1.00. The small

size of the particle, its format, and its stiffness are considered as the reasons for the low values of reduction factors compared to the ones found in previous studies.

- The elongation at rupture significantly decreased after the installation damage for both geotextiles under the impregnated and non-impregnated conditions. Moreover, the decreases when impregnated were more significant than the geotextile ones that were not impregnated. However, the results were very scattered, and no clear trend could be seen. Under the non-impregnation condition, the PET geotextile was the most affected, and the opposite occurred when impregnated (PP geotextile was the most affected).
- The secant tensile stiffness significantly increased after the installation damage procedure when the short-static and cyclic loading conditions were adopted. The long-static loading condition as responsible for significant decreases to the geotextiles' secant tensile stiffness regardless of the impregnation condition.
- The geotextiles' permittivity has shown contradictory results for either non-impregnated or impregnated conditions. After the installation damage, the PET geotextile presented decrease in the permittivity for most scenarios evaluated regardless of the impregnated condition. Despite the PP geotextile showed an increase in the permittivity values after the installation damage under non-impregnated condition, when impregnated it has shown different results for each asphalt emulsion and material present in the bottom layer – sometimes increasing and other decreasing.

The investigation shows that the geotextiles experienced an increase in their ultimate tensile strength and secant tensile stiffness after the impregnation, compounded by a reduction in its elongation at break and permittivity. Extreme caution must be taken due to the decrease in permittivity as it can help the development of water pressure inside the pavement structures. Moreover, the impregnation tends to increase the resistance of the geotextiles to installation damage, which acts on behalf of its application. However, designers must correctly consider the changes experienced by the geotextiles due to impregnation.

## REFERENCES

- Allen, T.M. and R.J. Bathurst (1994) Characterization of geosynthetic load-strain behavior after installation damage. *Geosynthetics International*, v. 1, n. 2, p. 181-99. DOI: 10.1680/gein.1.0008.
- ASTM (2005) ASTM D 6140: Standard Test Method to Determine Asphalt Retention of Paving Fabrics Used in Asphalt Paving for Full-Width Applications." West Conshohocken, PA: ASTM International.
- ASTM (2011) ASTM D 5035: Standard Test Method for Breaking Force and Elongation of Textile Fabrics (Strip Method). West Conshohocken, PA: ASTM International.
- ASTM (2012) ASTM D 5199: Standard Test Method for Measuring the Nominal Thickness of Geosynthetics. West Conshohocken, PA: ASTM International.
- ASTM (2013) ASTM D5/D5M - Standard Test Method for Penetration of Bituminous Materials. West Conshohocken, PA: ASTM International.
- ASTM (2016) ASTM D 6934: Standard Test Method for Residue by Evaporation of Emulsified Asphalt. West Conshohocken, PA: ASTM International.
- ASTM (2017a) ASTM D 4491: Standard Test Methods for Water Permeability of Geotextiles by Permittivity. West Conshohocken, PA: ASTM International.
- ASTM (2017b) ASTM D 7496: Standard Test Method for Viscosity of Emulsified Asphalt by Saybolt Furol Viscometer. West Conshohocken, PA: ASTM International.
- ASTM (2018) ASTM D 5261: Standard Test Method for Measuring Mass Per Unit of Geosynthetic Clay Liners. West Conshohocken, PA: ASTM International.



- Carlos, D.M.; J.R. Carneiro and M.L. Lopes (2019) Effect of different aggregates on the mechanical damage suffered by geotextiles. *Materials (Basel)*, v. 12, n. 24, p. 15. DOI: 10.3390/ma12244229. PMID:31861058.
- Carlos, D.M.; J.R. Carneiro; M. Pinho-Lopes et al. (2015) Effect of soil grain size distribution on the mechanical damage of nonwoven geotextiles under repeated loading. *International Journal of Geosynthetics and Ground Engineering*, v. 1, n. 1, p. 1-7. DOI: 10.1007/s40891-015-0011-9.
- Carneiro, J.R.; L.M. Morais; S.P. Moreira et al. (2013) Evaluation of the damages occurred during the installation of non-woven geotextiles. *Materials Science Forum*, v. 730-732, p. 439-444.
- Ching-Chuan, H. and C. Shuay-Luen (2006) Investigation of installation damage of some geogrid using laboratory tests, *Geosynthetics International*, v. 13, n. 1, p. 23-35. DOI: 10.1680/gein.2006.13.1.23.
- Correia, N.S. and J.G. Zornberg (2014) Influence of tack coat rate on the properties of paving geosynthetics. *Transportation Geotechnics*, v. 1, n. 1, p. 45-54. DOI: 10.1016/j.trgeo.2014.01.002.
- Correia, N.S.; J.G. Zornberg and B.S. Bueno (2014) Behavior of impregnated paving geotextiles: study of optimum tack coat rate. *Journal of Materials in Civil Engineering*, v. 26, n. 11, p. 04014077. DOI: 10.1061/(ASCE)MT.1943-5533.0001026.
- Domiciano, M.L.; E.C.G. Santos and J.L. Silva (2020) Geogrid mechanical damage caused by Recycled Construction and Demolition Waste (RCDW): influence of grain size distribution. *Soils and Rocks*, v. 43, n. 2, p. 231-246. DOI: 10.28927/SR.432231.
- Fleury, M.P.; M.A. Lima; E.C.G. Santos et al. (2023) Geotextile resistance to cyclic and static loading damage when impregnated with asphalt emulsion. *Construction & Building Materials*, v. 363, n. 129738, p. 14. DOI: 10.1016/j.conbuildmat.2022.129738.
- Gonzalez-Torre, I.; M.A. Calzada-Perez; A. Vega-Zamanillo et al. (2014) Damage evaluation during installation of geosynthetics used in asphalt pavements. *Geosynthetics International*, v. 21, n. 6, p. 377-386. DOI: 10.1680/gein.14.00025.
- Huang, C. and Z. Wang (2007) Installation damage of geogrids : influence of load intensity. *Geosynthetics International*, v. 14, n. 2, p. 65-75. DOI: 10.1680/gein.2007.14.2.65.
- Hufenus, R.; R. Rügger; D. Flum et al. (2005) Strength reduction factors due to installation damage of reinforcing geosynthetics. *Geotextiles and Geomembranes*, v. 23, n. 5, p. 401-424. DOI: 10.1016/j.geotextmem.2005.02.003.
- ISO (2007) ISO 10722: Geosynthetics - Index Test Procedure for the Evaluation of Mechanical Damage under Repeated Loading - Damage Caused by Granular Material. Geneva: ISO.
- Izadi, E.; T. Decraene; S. De Strijcker et al. (2018) A laboratory investigation on the impact resistance of a woven geotextile. *Geotextiles and Geomembranes*, v. 46, n. 1, p. 91-100. DOI: 10.1016/j.geotextmem.2017.10.003.
- Koerner, R.M. (2005) *Designing With Geosynthetics* (5th ed.). New Jersey: Person Education.
- Kondo, H.; T. Tanaka; T. Masuda et al. (1992) Aggin effects in 16 years on mechanica properties of commercial polymers. *Pure and Applied Chemistry*, v. 64, n. 12, p. 1945-1958. DOI: 10.1351/pac199264121945.
- Norambuena-Contreras, J. and I. Gonzalez-Torre (2015) Influence of geosynthetic type on retarding cracking in asphalt pavements. *Construction & Building Materials*, v. 78, p. 421-429. DOI: 10.1016/j.conbuildmat.2014.12.034.
- Obando-Ante, J. and E.M. Palmeira (2015) A laboratory study on the performance of geosynthetic reinforced asphalt overlays. *International Journal of Geosynthetics and Ground Engineering*, v. 1, n. 1, p. 1-11. DOI: 10.1007/s40891-014-0007-x.
- Paula, A.M.; M. Pinho-Lopes and M.L. Lopes (2004) Damage during installation laboratory test. Influence of the type of granular material. In German Geotechnical Society and The Technical University of Munich (orgs.) *3rd European Geosynthetics Conference*. Munich: German Geotechnical Society, p. 603-606.
- Pinho-Lopes, M. and M.L. Lopes (2014) Tensile properties of geosynthetics after installation damage. *Environmental Geotechnics*, v. 1, n. 3, p. 161-78. DOI: 10.1680/envgeo.13.00032.
- Pinho-Lopes, M.; A.M. Paula and M.L. Lopes (2018) Long-term response and design of two geosynthetics: effect of field installation damage. *Geosynthetics International*, v. 25, n. 1, p. 98-117. DOI: 10.1680/jgein.17.00036.
- Reinert, J. and R. Kerry Rowe (2021) Aging of geotextiles used in landfill applications - an initial study. In *4th Pan American Conference on Geosynthetics - GeoAmericas 2020*. Rio de Janeiro: IGS.
- Rowe, R.K.; S. Rimal and H. Sangam (2009) Ageing of HDPE geomembrane exposed to air, water and leachate at different temperatures Q. *Geotextiles and Geomembranes*, v. 27, n. 2, p. 137-151. DOI: 10.1016/j.geotextmem.2008.09.007.
- Wang, J.; F. Xiao; Z. Chen et al. (2017) Application of tack coat in pavement engineering. *Construction & Building Materials*, v. 152, p. 856-871. DOI: 10.1016/j.conbuildmat.2017.07.056.
- Wickert, F. (2003) *Fatores de Influência no Comportamento de Camadas Anti-Reflexão de Trincas com Geossintéticos*. Dissertation (master of science). Engenharia de Infra-Estrutura Aeronáutica, Instituto Tecnológico da Aeronáutica, São José dos Campos, SP. Available at: <<http://www.bdita.bibl.ita.br/>> (accessed 05/18/2023).
- Zamora-Barraza, D.; M.A. Calzada-Pérez; D. Castro-Fresno et al. (2011) Evaluation of anti-reflective cracking systems using geosynthetics in the interlayer zone. *Geotextiles and Geomembranes*, v. 29, n. 2, p. 130-136. DOI: 10.1016/j.geotextmem.2010.10.005.